4778–4787 *Nucleic Acids Research, 2010, Vol. 38, No. 14* *Published online 31 March 2010*
doi:10.1093/nar/gkq196

Global and local depletion of ternary complex limits translational elongation

Gong Zhang[1], Ivan Fedyunin[1,2], Oskar Miekley[1], Angelo Valleriani[2], Alessandro Moura[3,*] and Zoya Ignatova[1,*]

[1]Biochemistry, Institute of Biochemistry and Biology, University of Potsdam, Karl-Liebknecht-Str. 24-25, 14467 Potsdam, [2]Theory and Bio-Systems, Max Planck Institute of Colloids and Interfaces, 14424 Potsdam, Germany and [3]Institute of Complex Systems and Mathematical Biology, Dept. of Physics, University of Aberdeen, AB24 3UE Aberdeen, UK

Received December 23, 2009; Revised March 7, 2010; Accepted March 8, 2010

ABSTRACT

The translation of genetic information according to the sequence of the mRNA template occurs with high accuracy and fidelity. Critical events in each single step of translation are selection of transfer RNA (tRNA), codon reading and tRNA-regeneration for a new cycle. We developed a model that accurately describes the dynamics of single elongation steps, thus providing a systematic insight into the sensitivity of the mRNA translation rate to dynamic environmental conditions. Alterations in the concentration of the aminoacylated tRNA can transiently stall the ribosomes during translation which results, as suggested by the model, in two outcomes: either stress-induced change in the tRNA availability triggers the premature termination of the translation and ribosomal dissociation, or extensive demand for one tRNA species results in a competition between frameshift to an aberrant open-reading frame and ribosomal drop-off. Using the bacterial *Escherichia coli* system, we experimentally draw parallels between these two possible mechanisms.

INTRODUCTION

Faithful transmission of the genetic information from a messenger RNA (mRNA) to protein is crucial for normal cellular vitality and physiological functions. Ribosomes elongate the nascent peptide chain by sequential addition of amino acids in an mRNA template-directed manner by repetitive selection of aminoacylated-transfer RNA (aa-tRNA). Thereby the tRNA is repeatedly loaded with the cognate amino acid by ubiquitously expressed abundant aminoacyl-tRNA synthetases (aaRS) (1). The charged aa-tRNAs are delivered to the ribosome as a ternary complex (TC, aa-tRNA-EF-GTP) with the elongation factor [EF-Tu in bacteria and eEF1A (eEF1alpha) in eukaryotes] bound to GTP (2). Consequently, the concentration of the functional TCs is crucial for the rate of elongation at each codon.

The full set of 61 sense codons are read by specific isoaccepting tRNAs, which differ substantially in their concentration (3,4). This asymmetric tRNA abundance leads thereby to variations in the translation rate of each codon, and this results in a nonuniform speed of elongation along the mRNA (5): codons pairing to abundant tRNA species are translated faster compared to codons read by rare tRNAs (6). Bias in the usage of codons that pair to highly abundant tRNAs versus minor tRNAs can be a selection force for elongation speed (7,8), translation accuracy (2) or for higher fidelity of processes downstream of translation (5,9). Until now, codon usage bias (i.e. the variations in the frequency of usage of some synonymous codons versus others) has been used assuming that the codon usage patterns directly mirror the copy numbers and consequently the concentration of the cognate tRNA (4,10). Experimental quantification of the full set of tRNA species for two organisms, *Escherichia coli* and *Bacillus subtilis*, however, revealed deviations from the ideal proportionality between the tRNA concentration and codon usage (3,11). Moreover, in multicellular organisms, the tRNA concentrations vary among different tissues and stages of differentiation, in spite of the uniform codon usage and equal genomic copy number of the tRNAs in each cell (4,12). Similarly, in exponentially growing prokaryotic cells, the distributions of the tRNA concentrations have the potential to

*To whom correspondence should be addressed. Tel: +44 1224 272505; Fax: + 44 1224 273105; Email: a.moura@abdn.ac.uk
Correspondence may also be addressed to Zoya Ignatova. Tel: +49 331 977 5130; Fax: +49 331 977 5128; Email: ignatova@uni-potsdam.de

change very quickly (13) and certain rare codons are found to be unexpectedly translated at higher rates in spite of the low tRNA abundance (14,15).

Changes in the external environment modulate the abundance and concentration of the factors involved in the elongation cycle influencing thereby the dynamics of the elongation process. Limitations in the amino acids supply alter the pattern of the charged tRNA species (16,17). Variations in the macromolecular crowding of the cellular cytoplasm (e.g. in cells exposed to osmotic stress) influence macromolecular diffusion (18–20) thereby changing the rate of diffusion of the components participating in translation. Intriguingly, translational fidelity negatively correlates with the translational demand (21) and alterations in it (i.e. by variations of the protein expression profile) may alter the availability of some TCs.

To understand the dynamics and complexity of the elongation process, we developed a general model of translational elongation consisting of deterministic and stochastic parts. Analysis of the model revealed that perturbations in the delivery of the active TC to the ribosomes either by exhaustive demand for TC or diffusion limitations led to profound differences in the elongation rate of a single codon. Experimental analyses of translational profiles confirmed the predictions of our model; we observed that slower diffusion of TC in cells exposed to osmotic stress considerably increased the probability of premature termination of translation. In turn, an extensive demand for one single TC species during the overexpression of proteins with homopolymeric stretches was not compensated by an upregulated transcription of the cognate tRNA. This general model for translational elongation applies to all kingdoms of life, providing a systematic insight into mRNA elongation rate in response to diverse intrinsic (i.e. extensive request for one amino acid) and extrinsic (i.e. environmental changes) factors.

MATERIALS AND METHODS

tRNA quantification

Exon 1 of Htt with 53 CAG repeats was subcloned downstream of the GST moiety in the pGEX-6P-1 plasmid. The pure exon 1 with pathological repeats of 53Gln is highly aggregation-prone and the N-terminal GST-tag ensures its solubility throughout the expression cycle. Plasmids containing the insert were expressed in *E. coli* BL21(DE3) cells and cultured in LB medium at 37°C till OD = 0.6. Total tRNA was isolated as described elsewhere (22). The quality of tRNA was verified with the absorbance ratio $A_{260\,nm}/A_{280\,nm}$. cDNA was synthesized from the total tRNA samples using the *in vitro* reverse transcription kit (Fermentas) with random hexamer primers, and quantified in a real-time PCR cycler (StepOnePlus™ Real-Time PCR system, Applied Biosystems) with tRNA-specific primers. The tRNA concentration was normalized using the 5S rRNA concentration.

Polysomal profiles

The *E. coli* BL21(DE3) cells were cultivated in LB medium at 37°C and 220 r.p.m. till OD = 0.4 then harvested by centrifugation at 6000 r.p.m. for 5 min, resuspended in equal volume of M9 minimal medium and incubated further at 37°C till OD = 0.5. Cells were split into equal aliquots and to one aliquot NaCl was added to a final concentration of 300 mM (0.6 Osm) to exert osmotic stress. Cells were further cultured at 37°C for 20 min and their polysomes were isolated using the Cozzone's procedure with following modifications (23). The protoplasts from 100 ml culture were resuspended in 0.7 ml freshly prepared lysis buffer with 0.2% tritonX100, 10 U DNase I (RNase-free, Fermentas) and 1 U/μl Ribolock™ RNase inhibitor (Fermentas). The mixture was incubated 5 min at 37°C and clarified by centrifugation at 10 000*g* for 10 min at 4°C. Lysates containing the same amount of nucleic acids were layered onto 15–40% sucrose gradient in lysis buffer, and centrifuged for 2.5 h at 40 000 r.p.m. in SW65 rotor (Beckmann). The gradient was slowly pumped out and the $A_{260\,nm}$ was monitored by a flow-through UV spectrophotometer.

Numerical methods and stochastic simulations

The differential equations were solved in MatLab using non-stiff Runge Kutta method with a relative error tolerance of 10^{-7} (24).

The stochastic simulations were performed in a small cubic volume, which was equal to 1/10 of the typical *E. coli* volume (10^{-15} l) and contains the same density of ribosomes and TC as in *E. coli* cells. The numbers of ribosomes and TC in this volume were determined according to their concentrations in *E. coli* cells. The diffusion of the ribosomes is neglected, a simplification that is permitted because of the much larger size of the ribosomes (~3000 kDa) compared to the TC (~70 kDa). The ribosomes and TC are considered as spheres and are randomly located in this volume. In all three axes, the distance which a TC traverses in a Brownian diffusion can be described with the following probability distribution:

$$P(|d_x|,t) = \frac{1}{\sqrt{\pi D t}} e^{-\frac{d^2}{4Dt}} \quad (1)$$

where d_x is the distance projected on one axis, D is the diffusion coefficient and t is the time interval. We used periodic boundary conditions in the cubic spatial domain where the TC particles follow a Brownian motion and collisions are detected by calculating the distance between the TC and ribosomes.

An amino acid is delivered to the ribosome by an effective collision between TC and ribosomes. A collision event was detected when the distance between the centers of a TC and a ribosome becomes closer than the sum of their radii. However, only a small fraction of collisions was effective as determined by the effectiveness parameter: The collision effectiveness is adapted to the mean value of the translation rate derived from the experimental data in the deterministic model which comprises both structural details (the surface of the A-site entrance from the whole

ribosome surface) (25) and kinetic details on discrimination and tRNA-induced proofreading (2).

In an effective collision, a TC enters the A-site, therefore it is removed from the simulation volume and is replaced by another TC generated randomly in the volume, so that the TC concentration is maintained constant. To accelerate the simulation while minimizing the missing events, the time interval t was determined as 95% of the distance moved within one time interval, which was less than the radius of the TC. The simulations were programmed in VB.NET 2008.

A total of 53 661, 27 744 and 23 273 individual events were recorded in the simulations for cells grown in optimal conditions, in a medium with high osmolarity and by overexpressing polyGln-containing protein. The fitted parameters showed a significant deviation from the widely assumed exponential distribution ($a = 0.8393$, 95% confidential interval is 0.8307–0.8481 for normal conditions; $a = 0.8822$, 95% confidential interval is 0.8695–0.8951 for cells exposed to osmotic upshift; and $a = 0.8533$, 95% confidential interval is 0.8400–0.8669 for polyGln expressing cells) as justified by the comparison of the fitting parameters as ascertained by MatLab. The distribution of the waiting time of the ribosomes at the individual elongation events is fitted to the gamma function:

$$P(x) = \frac{1}{b^a \Gamma(a)} x^{a-1} e^{-x/b} \quad (2)$$

RESULTS

Deterministic model of translation elongation

The rate of translation of a single codon in the cell is determined by following four subsequent processes (Figure 1): (i) attachment of the amino acid to its cognate tRNA by the corresponding aaRS; (ii) aa-tRNA forms a TC-complex with GTP-bound elongation factor (EF-Tu in prokaryotes and eEF1A in eukaryotes); (iii) TC diffuses to a ribosome requesting it and tranfers the amino acid to the growing polypeptide chain, whereby the tRNA is released; and (iv) the GDP-bound elongation factor is regenerated into its GTP-bound state by EF-Ts (prokaryotes) or EF-1B/C (eukaryotes). All isoaccepting tRNAs for one amino acid are charged by their common aaRS with identical kinetic parameters (K_m and k_{cat}). The concentration of the aaRS is generally in proportion to the total concentration of its set of substrates, i.e. the full set of tRNAs mediating the transfer of one amino acid (3,26) with, as assumed here, homogeneous distribution of all components of the translational apparatus. Aside from methionine and tryptophan, all other amino acids are encoded by several synonymous triplets; therefore, the common aaRS is in a large excess over each tRNA isoacceptor, so we assume for all aaRS a constant concentration. The rate of formation of TC depends on the balance between the rate of supply (tRNA-charging and formation of the complex with the elongation factor) and demand of TC (consumption by the ribosomes, which is proportional to codon frequencies), and regeneration of EF-GTP (Figure 1). The active concentration of each of these components determines the rate of elongation of a single codon. Under conditions of non-limited amino acid supply, the mass balance equation for charged tRNA (aa-tRNA) concentration can be written as

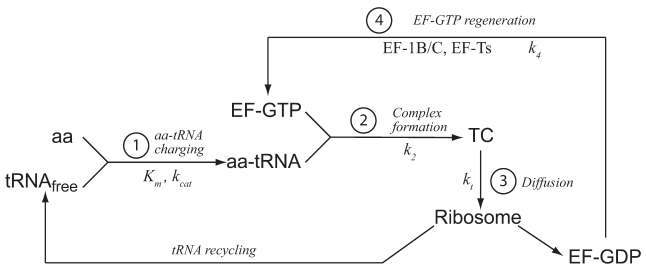

Figure 1. General scheme of translation elongation comprising four discrete processes.

$$\frac{d(f[tRNA])}{dt} = \frac{k_{cat}(1-f)[tRNA]}{K_m + (1-f)[tRNA]}[aaRS] - k_2[EF\text{-}GTP] f[tRNA] \quad (3)$$

Here [tRNA] and [aaRS] are the total concentration of a specific tRNA species and aaRS enzyme, respectively; f is the fraction of charged tRNA, k_{cat} and K_m are the enzymatic parameters of tRNA acylation catalyzed by the aaRS; k_2 is the rate constant of the complex formation between the charged tRNA with the EF [process (2), Figure 1]. The formation of the complex of EF-GTP with the aa-tRNA is very fast due to the high affinity and extremely high abundance of EF in both prokaryotes and eukaryotes (27). The concentration of TC ([TC]) depends on both TC formation and TC consumption with a rate constant k_t from a fraction of the ribosomes m which requests this tRNA isoacceptor [process (3), Figure 1]:

$$\frac{d[TC]}{dt} = k_2[EF\text{-}GTP] f[tRNA] - k_t[TC]m \quad (4)$$

The mass balance of the free tRNA can be given as

$$\frac{d[(1-f)[tRNA]]}{dt} = k_t[TC]m - \frac{k_{cat}(1-f)[tRNA]}{K_m + (1-f)[tRNA]}[aaRS] \quad (5)$$

The elongation factor delivers the aa-tRNA to the ribosomes and after initial stabilization of the complex by interaction of tRNA with mRNA, the GTPase activation and GTP-hydrolysis takes place. Cognate tRNA increases the rate of GTPase activation, whereas the mismatches in the codon–anticodon region with incorrect tRNA (near-cognate or non-cognate) impair this reaction (28). GTP-hydrolysis yields an inorganic phosphate and GDP in an EF-bound form. EF-GTP is regenerated by a second group of elongation factors with high abundance [EF-Ts in prokaryotes and eEF-1B/C in eukaryotes; process (4), Figure 1] and the mass balance is described by

$$\frac{d[EF\text{-}GDP]}{dt} = k_t[TC]m - k_4[EF\text{-}GDP][GTP] \quad (6)$$

where k_4 is the overall rate constant of EF-GTP regeneration. Furthermore, the mass balance of EF-GTP can be introduced as

$$\frac{d[\text{EF-GTP}]}{dt} = k_4[\text{EF-GDP}][\text{GTP}] - k_2[\text{EF-GTP}]f[t\text{RNA}] \quad (7)$$

The general model of translation elongation is valid for any organism. The EF-GTP regeneration is uniform for all TCs with a constant contribution to each single step of elongation independent of the TC species. In eukaryotes the recycling of eEF1A is much slower and shares rate controlling functions with processes (1) and (3), whereas in prokaryotes, the regeneration of EF-Tu-GDP is, compared to all other processes, relatively fast with only a minor contribution to the overall kinetics of elongation and can be therefore neglected (29,30). For prokaryotes the process (2) is much faster than (3) (Figure 1) and consequently the mass balance of TC can be simplified to

$$\frac{d(f[t\text{RNA}])}{dt} = \frac{k_{cat}(1-f)[t\text{RNA}]}{K_m+(1-f)[t\text{RNA}]}[\text{aaRS}] - k_t f[t\text{RNA}]m \quad (8)$$

As the elongation factor is in large excess over each tRNA species, the concentration of the TC is directly proportional to the concentration of the free tRNA (26). In turn, the average waiting time of the ribosome for a cognate TC will be

$$\tau = \frac{1}{k_t f[t\text{RNA}]} \quad (9)$$

To illustrate the outcomes of Equation (8), we took as an example $tRNA_2^{Gln}$ which in *E. coli* pairs solely to the CAG codon encoding glutamine (Gln). Under non-limiting Gln supply, the kinetic parameters of the aaRS enzyme are $k_{cat} = 3.20 \pm 0.48\,s^{-1}$ and $K_m = 0.31 \pm 0.09\,\mu M$ (for tRNA) (31); the concentrations of the tRNA and glutamyl-tRNA synthetase (GlnRS) are 1.46×10^{-6} M and 2.79×10^{-6} M, respectively (3,26). The maximal concentration of the ribosomes which could simultaneously request the CAG codon can be estimated from the CAG codon usage and is calculated to be 6.88×10^{-7} M. At steady state, where 80% of the tRNA is charged ($f = 0.8$) (16), Equation (8) can be then solved for k_t; the resulting value is 5.39×10^6 $s^{-1}\,mol^{-1}\,l$. Consequently, the translation rate (r_t) is predicted to be: $r_t = k_t f[t\text{RNA}]m = 4.33 \times 10^{-6}$ $mol\,l^{-1}s^{-1}$, or 6.3 CAG codons/ribosome/s. This result is consistent with the experimentally measured translation rate in *E. coli* (4.2–21.6 codons/s) (32).

TC can be globally exhausted by excessive demand

By expression of proteins with homopolymeric amino acid runs or repetitive sequences, or by heterologous and homologous overexpression of proteins, the translation demand of specific TC species may significantly increase, thereby increasing the waiting time of the ribosome for the cognate TC. The presence of additional homopolymeric codon stretches (here exemplified by CAG runs) can be modeled by including an additional term in Equation (8):

$$\frac{d(f[t\text{RNA}])}{dt} = \frac{k_{cat}(1-f)[t\text{RNA}]}{K_m+(1-f)[t\text{RNA}]}[\text{aaRS}] - k_t f[t\text{RNA}](m+m_{CAG}) \quad (10)$$

where the m_{CAG} is the concentration of the fraction from the ribosome pool involved in the translation of proteins with homopolymeric Gln stretches or of overexpressed proteins rich in CAG codons. Solving this equation numerically using the Runge–Kutta integration method (exemplified again for *E. coli* $tRNA_2^{Gln}$) revealed that because of the excessive demand, the concentration of TC-$tRNA_2^{Gln}$ decreased significantly within <0.5 s (Figure 2A). This transition time corresponded to the time needed to translate 2–3 consecutive codons. The waiting time of the ribosomes increased parallel to the number of ribosomes simultaneously requesting the same TC (Figure 2B). The effect is inversely correlated

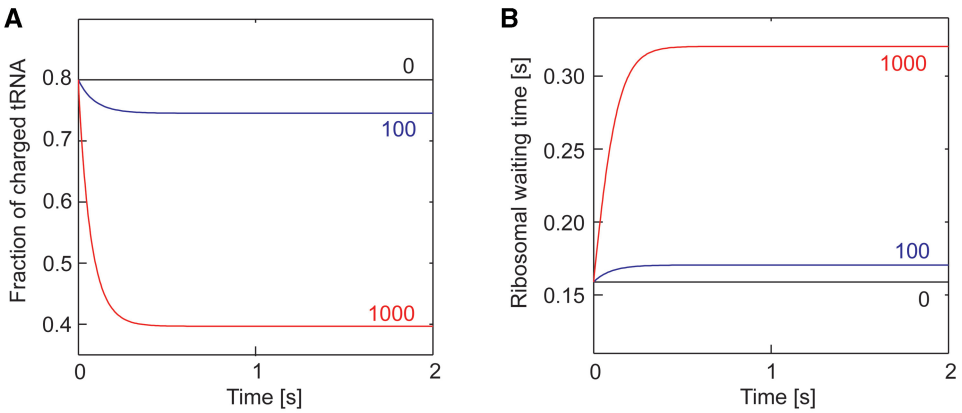

Figure 2. Global depletion of TC exemplified with the demand of $tRNA_2^{Gln}$. (**A**) The fraction of charged TC decreased by its simultaneous request by m_{CAG} (0, 100, 1000 ribosomes). The numbers 100 and 1000 indicate that 0.24 and 2.4 times more ribosomes are translating CAG repeats than in the isolated CAG codons which are present normally in the *E. coli* genome. (**B**) The increase of the waiting time of the ribosomes for translating a single CAG codon parallels the increase of the concentration of the ribosomes that are involved in the translation of polyGln stretches (m_{CAG} = 0, 100, 1000).

to the codon usage: the depletion and the new steady state is established faster for tRNAs pairing to rare codons than to frequently used ones (Figure S1, Table S1). Essential proteins for growth are highly abundant and their mRNAs are enriched in codons that pair to major tRNAs and are thus optimized for fast translation speed (3,33). The slower depletion of the major tRNAs will ensure a sufficient level of expression of essential genes even in a conditions of high demand of the particular cognate tRNA.

Here, we assumed that the tRNA concentration of each species remains constant. However, the cell can modulate tRNA abundance according to the demand and specificity of the protein pattern (12,34). To investigate whether the $tRNA_2^{Gln}$ is upregulated when it is highly requested in translation, we measured its cellular concentration in cells overexpressing model proteins with a consecutive polyglutamine (polyGln) stretch built of CAG-codons only. We used the GST-fusion of Huntingtin exon 1 with 53 Gln (GST-Htt53Gln) which is implicated in Huntington's disease. To experimentally simulate a large demand for $tRNA_2^{Gln}$, we expressed the GST-Htt53Gln on a plasmid with a high-copy number which produced >2500 mRNA copies simultaneously. Using quantitative RT-PCR under a confidence level of 95%, we could not detect an upregulation of the $tRNA_2^{Gln}$ (Figure 3), suggesting that an increased demand for one TC is not compensated by a transcriptional upregulation of the corresponding tRNA species; the level of the tRNA in the cell remained unchanged which in turn confirmed our assumption of constant concentration of $tRNA_2^{Gln}$.

TC is locally depleted in the vicinity of the ribosomes translating homopolymeric stretches

To address the question of whether there is a concentration gradient built in the vicinity of a ribosome repeatedly translating one codon (i.e. by translation of homopolymeric stretches), we extended the model with the spatial diffusion of the TC complexes around ribosomes translating repetitive sequences. The TC is delivered to the ribosomes solely by passive diffusion, which we assumed here to follow Fick's law. Even though the cytosol is highly crowded, both proteins and RNA particles diffuse in a typical Brownian manner albeit with a slower diffusion coefficients (20,35). We also assumed that each TC is generated away from the aa-tRNA-binding site, A-site, of the ribosome and the diffusion is isotropic. One evidence for this assumption is that aaRS have not been co-isolated or identified in the close proximity of the A-site and even though they might be in a close proximity to the ribosomes (36) there is still a diffusion path for the TC to the A-site. Approximating the ribosome as a sphere, the diffusion of the TC in its vicinity can be described as

$$\frac{\partial c}{\partial t} = D\nabla^2 c = D\frac{1}{r^2}\frac{\partial}{\partial r}\left(r^2\frac{\partial c}{\partial r}\right) \quad (11)$$

where D is the diffusion coefficient, $c = c(r,t)$ is the concentration of TC as a function of position and time and r is the distance to the center of the ribosome. We used a spherical coordinate system with the ribosome at the origin. At the radius where the TC collides with ribosome $r = a$ and $c = c_0$, whereas far away from the ribosome $r = \infty$, $c = c_\infty$. We solved Equation (11) in the case of *E. coli* with the following setup: $a = 14$ nm, the diffusion coefficient of TC is $2.569 \times 10^{-12}\,m^2/s$ (37). At steady state, $\partial c/\partial t = 0$. Solving the Equation (11) reveals the radial profile of TC concentration (Figure 4A):

$$c(r) = c_\infty - \frac{1}{r}a(c_\infty - c_0) \quad (12)$$

The supply rate of TC by diffusion is given by

$$I = D\left.\frac{\partial c}{\partial r}\right|_{r=a} \cdot 4\pi a^2 = 4\pi a D(c_\infty - c_0) \quad (13)$$

and the consumption rate of TC in translation is

$$I = \frac{k_t f[\mathrm{tRNA}]}{N_A} = \frac{k_t c_0}{N_A} \quad (14)$$

where N_A is Avogadro's constant. At steady state, the TC consumption rate is equal to the supply rate. Solving the equations reveals the local depletion factor (L):

$$L = \frac{c_0}{c_\infty} = \frac{1}{(k_t/4\pi a \mathrm{D} N_A)+1} \quad (15)$$

The outcome of this analysis shows that $tRNA_2^{Gln}$ can be locally depleted due to diffusion (Figure 4A), which limits additionally the rate of translation of consecutive stretches (here polyGln). Importantly, local depletion may also occur in the vicinity of ribosomes translating isolated CAG codons; however, the effect is much stronger for ribosomes involved in the translation of consecutive polyGln stretches. Considering the effect of the local depletion on the ribosomes translating repetitive stretches, the Equation (10) is modified by a factor Lm_{CAG}:

$$\frac{\mathrm{d}(f[t\mathrm{RNA}])}{\mathrm{d}t} = \frac{k_{cat}(1-f)[t\mathrm{RNA}]}{K_m+(1-f)[t\mathrm{RNA}]}[\mathrm{aaRS}] - k_t f[t\mathrm{RNA}](m+Lm_{CAG}) \quad (16)$$

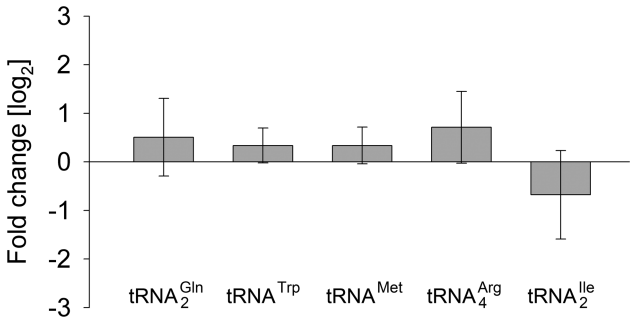

Figure 3. During the expression of proteins with polyGln stretches the concentration of the highly requested free $tRNA_2^{Gln}$ isoacceptor remained unchanged as measured by real-time qRT-PCR. Values are expressed as fold change (log_2; mean ± SD) compared to the control cells expressing only background, chromosomally encoded proteins. $tRNA^{Trp}$, $tRNA^{Met}$, $tRNA_4^{Arg}$ and $tRNA_2^{Ile}$ were used as controls showing also no differences to the control conditions.

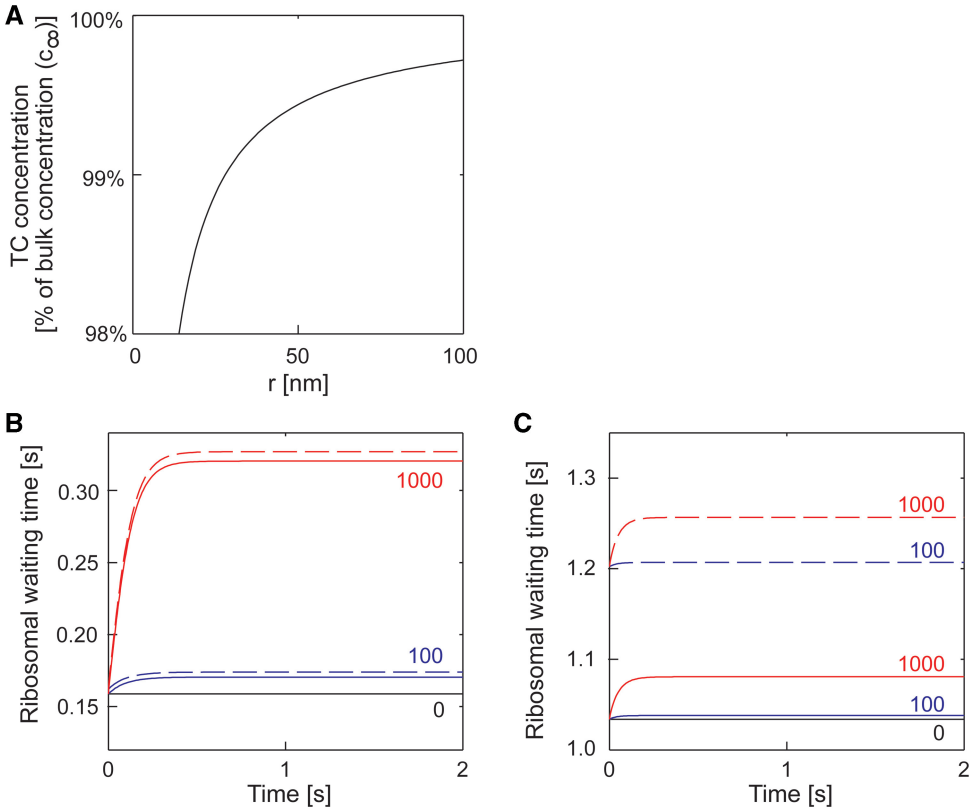

Figure 4. Local depletion of the TC increases the waiting time of a ribosome at a single codon. (**A**) A radial profile of TC concentration in the vicinity of a ribosome translating CAG repeats at steady state. (**B**) Waiting time of the ribosomes translating CAG repeats (dashed lines) slightly increased compared to the ribosomes translating isolated CAG codons (solid lines). The simulations were performed assuming that m_{CAG} [0 (black), 100 (blue) or 1000 (red)] ribosomes are simultaneously translating polyGln stretches in one *E. coli* cell. (**C**) Exposure of the cells to osmotic stress (0.6 Osm) severely increased the waiting time of the ribosomes translating isolated CAG codons (solid lines) and CAG repeats (dashed lines).

Consequently, local depletion will affect the waiting time [Equation (9)]:

$$\tau_L = \frac{\tau}{L} = \frac{(k_t/4\pi a D N_A)+1}{k_t f[t\mathrm{RNA}]} \quad (17)$$

Under optimal growth conditions, the local depletion has minor contributions to the extension of the waiting time of the ribosomes ($L = 0.98$) (Figure 4B).

External stress generally leads to changes in the cell volume and solute composition in the cytosol (38) and alters the macromolecular crowding (20). In the case of osmotic upshift in the cellular environment, the primary response of the cell is a loss of large amounts of water, which in turn causes an increase in the macromolecular concentration in the cytosol and consequently alters the diffusion properties of proteins (18,19). To address the effect of perturbed diffusion of TC on translation elongation, we next performed the simulations in conditions of osmotic stress (Figure 4C). We chose mild osmotic stress (0.6 Osm) in which diffusion is still permitted albeit much slower; the diffusion coefficient of the ~70 kDa TC complex decreased from $2.569 \times 10^{-12}\,m^2\,s^{-1}$ (37) to $0.32 \times 10^{-12}\,m^2\,s^{-1}$ on osmotic upshift to 0.6 Osm imposed by NaCl (18,19). The analysis suggests that even mild osmotic upshift and moderately enhanced macromolecular crowding has a tremendous effect on the waiting time of ribosomes for the cognate TC (Figure 4C) and will considerably delay the translation of a single codon because of an increased global depletion of TC ($L = 0.98$ at 0 Osm, $L = 0.86$ at 0.6 Osm and $L = 0.41$ at 1.45 Osm).

Stochastic distribution of the individual elongation events

Intracellular reactions occur far from thermodynamic equilibrium and the relatively low total number of each molecular species in the cell suggests that fluctuations can be significant and are likely to play an important role in the elongation dynamics. To address this, we propose a stochastic model to describe the individual translation elongation events. For simulation of the movement of passively diffusing TC we used Brownian random-walker model (Supplementary Methods in Supplementary Data) that allowed recording of the waiting time of ribosomes in individual elongation events (Figure 5A). Intriguingly, the best fit of the distribution of the individual ribosomal waiting times is given by the gamma function rather than the exponential function (Figure 5A, Supplementary Methods in Supplementary Data). The interactions between two of the ribosomal proteins (L7/L12) with the elongation factor (EF-Tu) promote

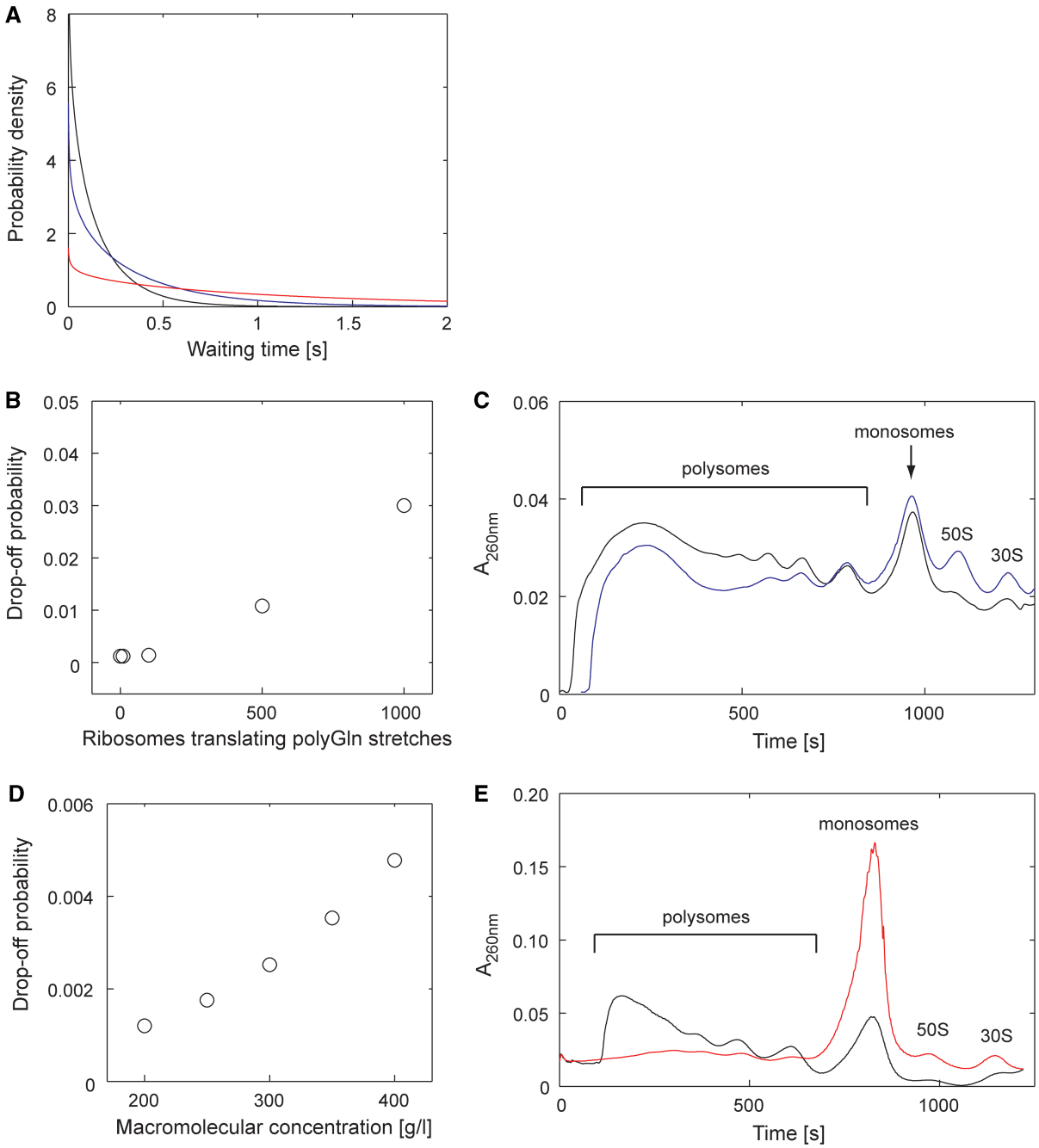

Figure 5. The probability of aberrant translation increased by extensive demand of one TC species or global alterations in the TC concentration. (**A**) Gamma fit of the distribution of the waiting time of ribosomes under optimal growth conditions (black), osmotic stress (red) and overexpressed polyGln protein with $m_{CAG} = 1000$ (blue). (**B**) Large number of ribosomes simultaneously translating polyGln stretches enhances the probability of ribosomal disassembly. (**C**) Polysomal profile of *E. coli* cells growing in normal balanced medium (black) and overexpressing Htt exon 1 with 53Gln (blue). To exclude any effect of the plasmid backbone, the control cells were transformed with the empty vector. The peaks corresponding to single ribosomal subunits are designated 30S and 50S, monosomes as M, and peaks representing mRNA occupied by two and more ribosomes are marked as polysomes. (**D**) Increased molecular crowding by an external osmotic upshift decreases the diffusion coefficient of the TC and subsequently increases the ribosomal drop-off. The macromolecular concentration and its influence on the diffusion properties on the macromolecules was calculated as described (20). Note that in the simulations in (B) and (D), the competition of the release factor for the A-site of the transiently paused ribosomes is considered. (**E**) Polysomal profile of *E. coli* cells grown in normal balanced medium (black) and in medium with osmolarity of 0.6 Osm (red). 30S and 50S denote the peaks corresponding to dissociated small and large subunits, respectively.

ternary complex binding to the ribosome (39) and are most likely the reason for the observed gamma distribution. Additionally, we performed a series of simulations with different parameters to address their impact on the waiting time: ribosomal concentration has no influence on the distribution, whereas the scale (parameter *b*) shows an inverse correlation to the tRNA concentration and the diffusion coefficient (Figure S2). In turn, the probability

density function (parameter a) positively correlates with the diffusion coefficient, and increases slightly only at a very low TC concentration (Supplementary Figure S2). In all cases, $a < 1$ suggesting a significant deviation from the exponential distribution exists independent of the simulation setup.

Our predictions clearly suggest that both global and local depletion of TC extend the average residence time of the ribosomes at a single codon (Figure 5A). Two outcomes are possible in the case of an aberrant ribosomal stalling in the cell: (i) frameshift to a new open-reading frame (40) or (ii) premature termination of synthesis (41). There is no clear, experimentally determined cutoff in the residence time of the ribosomes to distinguish between the two processes. Radioactive measurements of the drop-off frequency at leucine-encoding codons (42) suggest an average time of 1.17 s; however, it cannot be differentiated among the five tRNA species pairing to the six Leu-encoding codons. The frameshifting at evolutionary non-programmed sites occurs infrequently with a quite low rate below 3×10^{-5} per codon, which is two orders of magnitude lower than the natural ribosomal drop-off (43), suggesting that concomitantly to the ribosomal dissociation frameshift will occur albeit with significantly lower frequency. The frameshift probability is non-uniform among the codons, preferably occurring at codons read by minor tRNAs (44), whereas equal selection of all tRNAs at the ribosomes (45) will favor the uniform probability of ribosomal dissociation independent of the codon. Therefore, hereafter for simplicity we refer to any aberrant outcome of the elongation as ribosome dissociation, which for some intrinsically frameshifting-prone codons might equal frameshift probability. The probability of premature termination of the elongation (P_d) can then be expressed as

$$P_d = \int_{\tau_d}^{\infty} P(t)dt \quad (18)$$

Under optimal growth conditions, the global depletion caused by excessive demand of $tRNA_2^{Gln}$ is significantly influenced by the number of ribosomes simultaneously requesting the same TC (Figure 5A and B), whereas under osmotic stress, altered diffusion properties of TC (Figure 5A and D) add to this effect and the average waiting time of the ribosomes increases. The ribosomes stalled at a nonstop codon can be rescued in two ways in bacteria: (i) transfer-messenger RNA (tmRNA or SsrA) releases the stalled ribosomes by trans-translational tagging of the nascent chain by 10-amino-acid tag and targeting it to degradation (46), or (ii) release factors coordinate the hydrolysis of the stalled nascent chain (47). As the tmRNA is complexed with the elongation factor its diffusion will be similarly influenced as all TCs by the increased macromolecular crowding in the cell. The release factor ($\sim$40 kDa), however, is smaller than the TC ($\sim$70 kDa) and its diffusion mobility will be affected to a lower extent in the more crowded environment (20); the higher mobility of release factor in osmotically stressed cells will increase the probability to encounter stalled ribosomes. Therefore, in the stochastic simulations, we considered the competition between the release factor and the cognate TC for the A-site of the aberrantly stalled ribosomes (Figure 5D).

To examine whether the frequency of premature translational termination is influenced by an extensive demand of $tRNA_2^{Gln}$ or altered macromolecular diffusion, we compared the translational activity by examining the polysomal profiles of exponentially growing *E. coli* cells with cells overexpressing GST-Htt53Gln (Figure 5C) and *E. coli* cells subjected to osmotic upshift (Figure 5E). mRNA is actively translated by multiple ribosomes, i.e. polysomes, that can be separated on sucrose density gradients. The translation profiles of polyGln protein expressing cells are dominated by the polysome fraction similar to the profiles of the cells cultured in balanced medium (Figure 5C). The presence of peaks of single ribosomal subunits account for a small fraction of dissociated ribosomes (Figure 5C) as also predicted by the model (Figure 5B). In contrast, there was a dramatic shift of ribosomes from the polysomal region into single dissociated subunits or monosome following osmotic upshift (Figure 5E). The peaks of the single subunits account for the translational drop-off, whereas the enriched monosomal peak corresponds to ribosomal run-off (Figure S3); osmotic stress inhibits translational initiation resulting in ribosomal run-off (48,49).

DISCUSSION

Our model provides a general theoretical framework to predict the global elongation rate composed of single elongation steps under dynamic circumstances, e.g. including changes in cellular environment under stress conditions, exhaustive demand for one amino acid, tRNA availability by using both deterministic and stochastic approaches. It sheds light on the kinetics of the single elongation steps, which are by their transient nature difficult to track experimentally. Here, we present an example for translation in prokaryotes; however, the general model (Figure 1) can be applied to any organism and cell type provided that an adequate experimental data set for the system available, e.g. tRNA and elongation factor concentrations, kinetic properties of the cognate aaRS. Currently, the lack of quantitative data sets of eukaryotic tRNAs hinders the predictions for eukaryotic systems, even though the kinetic data of EF-GTP regeneration is currently available (29). The suggestion of structural organization of the eukaryotic protein synthesis machinery in large complexes which are spatially localized by linkage with the cytoskeletton and endoplasmic reticulum (36) would require a change in the parameters in the stochastic simulation and in turn would demand extremely high computational power. However, there is still a distance between aaRS and the A-site of the ribosome, which each TC complex has to pass in a passive Brownian diffusion. Furthermore, the model is not limited to external stress types (osmotic, temperature and oxidative) that change the solute composition and consequently alter the diffusion properties of the ternary complex. When cells are starved, the restricted supply of

an amino acid severely limits the availability of the cognate ternary complex and the charging of the tRNA isoacceptors [process (i), Figure 1] becomes rate limiting. The charging pattern within one set of isoacceptors for the same amino acid differs: the charged level of some tRNAs approaches zero and remains high for others (17). tRNAs that retain the charging pattern are enriched in genes involved in the amino acid biosynthesis suggested to be a regulatory loop to counteract the starvation (17). The differential charging pattern within one isoacceptor family will result in variations in the *f*-value for each tRNA species increasing the complexity of the Equation (1); however, the principle remains unaltered.

A crucial feature of the model is that it can predict a ribosomal stalling at single codons and a probability of aberrant translational outcome (i.e. frameshift and premature termination of the translational elongation). Both global and local depletion of TC influence the residence time of the ribosomes at a single codon. In the case of a local depletion, the flow of a TC is altered owing to the repeated request of a single TC (i.e. by translation of homopolymeric stretches) in the vicinity of the ribosome which leads to an unexpected, non-naturally programmed pause in translation. As the diffusion properties and concentrations of all other TCs are unaltered, there is a high probability that an incorrect TC (near-cognate or non-cognate) can compete for binding to the A-site. During such pause, the alignment of the near-cognate and non-cognate TC to at least two nucleotides from the mRNA would cause a shift in the open-reading frame creating thereby a completely new amino acid sequence (40). Interestingly, many homopolymeric stretches show a high tendency to frameshift *in vivo* resulting in a more severe disease phenotype: in one cell a small fraction CAG repeats encoding polyGln proteins frameshift to polyalanine sequences encoded by GCA-stretches (50). In stretches consisting of repetitive slow-translating codons, this effect can be substantially enhanced: even in stretches as short as only two codons the frameshifting can be significant (51,52).

In contrast to the case of local depletion that has consequences for only one TC, altered cellular diffusion of macromolecules caused by external stress conditions affects the diffusion of all TC species equally, leading to their global depletion. As suggested by our results poor availability of any TC for translation would transiently stall the ribosomes and trigger their premature dissociation. Consistently, hypertonic stress disrupts initiation and elongation steps resulting in synthesis of incomplete polypeptides (48,49).

The finding that low TC availability can lead to two quite different outcomes, frameshifting or premature termination, suggests the feasibility of investigating the dynamics of translational elongation using our predictions. Regulation of the elongation cycles during translation plays an important role in the cell to control the cell cycle and to adjust proteome composition to acute needs. As our model can adequately predict the elongation kinetics under dynamic conditions, it bears the potential to understand the mechanisms of translational elongation, their dynamics and sensitivity to environmental factors in a systematic way.

SUPPLEMENTARY DATA

Supplementary Data are available at NAR Online.

ACKNOWLEDGEMENTS

We thank Sam Miller (Univ. of Aberdeen) for the critical reading of the manuscript, Salma Balazadeh and Bernd Müller-Röber (Molecular Biology, University Potsdam) for the help with the qRT-PCR.

FUNDING

The SysMO (grant Kosmobac to Z.I. and A.M.); Deutsche Forschungsgemeinschaft (grant IG 73/10-1 to Z.I.). Funding for open access charge: BBSRC (to A.M.) and DFG (to Z.I).

Conflict of interest statement. None declared.

REFERENCES

1. Ibba,M. and Soll,D. (2000) Aminoacyl-tRNA synthesis. *Annu. Rev. Biochem.*, **69**, 617–650.
2. Rodnina,M.V. and Wintermeyer,W. (2001) Ribosome fidelity: tRNA discrimination, proofreading and induced fit. *Trends Biochem. Sci.*, **26**, 124–130.
3. Dong,H., Nilsson,L. and Kurland,C.G. (1996) Co-variation of tRNA abundance and codon usage in Escherichia coli at different growth rates. *J. Mol. Biol.*, **260**, 649–663.
4. Ikemura,T. (1985) Codon usage and tRNA content in unicellular and multicellular organisms. *Mol. Biol. Evol.*, **2**, 13–34.
5. Zhang,G., Hubalewska,M. and Ignatova,Z. (2009) Transient ribosomal attenuation coordinates protein synthesis and co-translational folding. *Nat. Struct. Mol. Biol.*, **16**, 274–280.
6. Lavner,Y. and Kotlar,D. (2005) Codon bias as a factor in regulating expression via translation rate in the human genome. *Gene*, **345**, 127–138.
7. Makhoul,C.H. and Trifonov,E.N. (2002) Distribution of rare triplets along mRNA and their relation to protein folding. *J. Biomol. Struct. Dyn.*, **20**, 413–420.
8. Sorensen,M.A., Kurland,C.G. and Pedersen,S. (1989) Codon usage determines translation rate in Escherichia coli. *J. Mol. Biol.*, **207**, 365–377.
9. Komar,A.A. (2009) A pause for thought along the co-translational folding pathway. *Trends Biochem. Sci.*, **34**, 16–24.
10. Andersson,S.G. and Kurland,C.G. (1990) Codon preferences in free-living microorganisms. *Microbiol Rev.*, **54**, 198–210.
11. Kanaya,S., Yamada,Y., Kudo,Y. and Ikemura,T. (1999) Studies of codon usage and tRNA genes of 18 unicellular organisms and quantification of Bacillus subtilis tRNAs: gene expression level and species-specific diversity of codon usage based on multivariate analysis. *Gene*, **238**, 143–155.
12. Dittmar,K.A., Goodenbour,J.M. and Pan,T. (2006) Tissue-specific differences in human transfer RNA expression. *PLoS Genet.*, **2**, e221.
13. Rocha,E.P. (2004) Codon usage bias from tRNA's point of view: redundancy, specialization, and efficient decoding for translation optimization. *Genome Res.*, **14**, 2279–2286.
14. Bonekamp,F., Dalboge,H., Christensen,T. and Jensen,K.F. (1989) Translation rates of individual codons are not correlated with tRNA abundances or with frequencies of utilization in Escherichia coli. *J. Bacteriol.*, **171**, 5812–5816.
15. Curran,J.F. and Yarus,M. (1989) Rates of aminoacyl-tRNA selection at 29 sense codons in vivo. *J. Mol. Biol.*, **209**, 65–77.

16. Dittmar,K.A., Sorensen,M.A., Elf,J., Ehrenberg,M. and Pan,T. (2005) Selective charging of tRNA isoacceptors induced by amino-acid starvation. *EMBO Rep.*, **6**, 151–157.
17. Elf,J., Nilsson,D., Tenson,T. and Ehrenberg,M. (2003) Selective charging of tRNA isoacceptors explains patterns of codon usage. *Science*, **300**, 1718–1722.
18. Konopka,M.C., Sochacki,K.A., Bratton,B.P., Shkel,I.A., Record,M.T. and Weisshaar,J.C. (2009) Cytoplasmic protein mobility in osmotically stressed Escherichia coli. *J. Bacteriol.*, **191**, 231–237.
19. van den Bogaart,G., Hermans,N., Krasnikov,V. and Poolman,B. (2007) Protein mobility and diffusive barriers in Escherichia coli: consequences of osmotic stress. *Mol. Microbiol.*, **64**, 858–871.
20. Zimmerman,S.B. and Minton,A.P. (1993) Macromolecular crowding: biochemical, biophysical, and physiological consequences. *Annu. Rev. Biophys. Biomol. Struct.*, **22**, 27–65.
21. Honigman,A., Falk,H., Mador,N., Rosental,T. and Panet,A. (1995) Translation efficiency of the human T-cell leukemia virus (HTLV-2) gag gene modulates the frequency of ribosomal frameshifting. *Virology*, **208**, 312–318.
22. Cayama,E., Yepez,A., Rotondo,F., Bandeira,E., Ferreras,A.C. and Triana-Alonso,F.J. (2000) New chromatographic and biochemical strategies for quick preparative isolation of tRNA. *Nucleic Acids Res.*, **28**, E64.
23. Cozzone,A. and Donini,P. (1973) Turnover of polysomes in amino acid-starved Escherichia coli. *J. Mol. Biol.*, **76**, 149–162.
24. Dormand,J.R.P. and Prince,P.J. (1980) A family of embedded Runge–Kutta formulae. *J. Comp. Appl. Math.*, **6**, 19–26.
25. Steitz,T.A. (2008) A structural understanding of the dynamic ribosome machine. *Nat. Rev. Mol. Cell Biol.*, **9**, 242–253.
26. Ishihama,Y., Schmidt,T., Rappsilber,J., Mann,M., Hartl,F.U., Kerner,M.J. and Frishman,D. (2008) Protein abundance profiling of the Escherichia coli cytosol. *BMC Genomics*, **9**, 102.
27. Roy,H., Becker,H.D., Mazauric,M.H. and Kern,D. (2007) Structural elements defining elongation factor Tu mediated suppression of codon ambiguity. *Nucleic Acids. Res.*, **35**, 3420–3430.
28. Rodnina,M.V., Gromadski,K.B., Kothe,U. and Wieden,H.J. (2005) Recognition and selection of tRNA in translation. *FEBS Lett.*, **579**, 938–942.
29. Janssen,G.M. and Moller,W. (1988) Kinetic studies on the role of elongation factors 1 beta and 1 gamma in protein synthesis. *J. Biol. Chem.*, **263**, 1773–1778.
30. Pittman,Y.R., Valente,L., Jeppesen,M.G., Andersen,G.R., Patel,S. and Kinzy,T.G. (2006) Mg2+ and a key lysine modulate exchange activity of eukaryotic translation elongation factor 1B alpha. *J. Biol. Chem.*, **281**, 19457–19468.
31. Uter,N.T. and Perona,J.J. (2004) Long-range intramolecular signaling in a tRNA synthetase complex revealed by pre-steady-state kinetics. *Proc. Natl Acad. Sci. USA*, **101**, 14396–14401.
32. Sorensen,M.A. and Pedersen,S. (1991) Absolute in vivo translation rates of individual codons in Escherichia coli. The two glutamic acid codons GAA and GAG are translated with a threefold difference in rate. *J. Mol. Biol.*, **222**, 265–280.
33. Zhang,G. and Ignatova,Z. (2009) Generic algorithm to predict the speed of translational elongation: Implications for protein biogenesis. *PLoS ONE*, **4**, e5036.
34. Kanduc,D. (1997) Changes of tRNA population during compensatory cell proliferation: differential expression of methionine-tRNA species. *Arch. Biochem. Biophys.*, **342**, 1–5.
35. Golding,I. and Cox,E.C. (2004) RNA dynamics in live Escherichia coli cells. *Proc Natl Acad Sci USA*, **101**, 11310–11315.
36. Deutscher,M.P. (1984) The eucaryotic aminoacyl-tRNA synthetase complex: suggestions for its structure and function. *J. Cell Biol.*, **99**, 373–377.
37. Fluitt,A., Pienaar,E. and Viljoen,H. (2007) Ribosome kinetics and aa-tRNA competition determine rate and fidelity of peptide synthesis. *Comput. Biol. Chem.*, **31**, 335–346.
38. Bolen,D.W. and Rose,G.D. (2008) Structure and energetics of the hydrogen-bonded backbone in protein folding. *Annu. Rev. Biochem.*, **77**, 339–362.
39. Kothe,U., Wieden,H.J., Mohr,D. and Rodnina,M.V. (2004) Interaction of helix D of elongation factor Tu with helices 4 and 5 of protein L7/12 on the ribosome. *J. Mol. Biol.*, **336**, 1011–1021.
40. Farabaugh,P.J. (1996) Programmed translational frameshifting. *Microbiol. Rev.*, **60**, 103–134.
41. Cruz-Vera,L.R., Hernandez-Ramon,E., Perez-Zamorano,B. and Guarneros,G. (2003) The rate of peptidyl-tRNA dissociation from the ribosome during minigene expression depends on the nature of the last decoding interaction. *J. Biol. Chem.*, **278**, 26065–26070.
42. Menninger,J.R. (1976) Peptidyl transfer RNA dissociates during protein synthesis from ribosomes of Escherichia coli. *J. Biol. Chem.*, **251**, 3392–3398.
43. Kurland,C.G. (1992) Translational accuracy and the fitness of bacteria. *Annu. Rev. Genet.*, **26**, 29–50.
44. Vimaladithan,A. and Farabaugh,P.J. (1994) Special peptidyl-tRNA molecules can promote translational frameshifting without slippage. *Mol. Cell Biol.*, **14**, 8107–8116.
45. Ledoux,S. and Uhlenbeck,O.C. (2008) Different aa-tRNAs are selected uniformly on the ribosome. *Mol. Cell*, **31**, 114–123.
46. Withey,J.H. and Friedman,D.I. (2003) A salvage pathway for protein structures: tmRNA and trans-translation. *Annu. Rev. Microbiol.*, **57**, 101–123.
47. Hirokawa,G., Demeshkina,N., Iwakura,N., Kaji,H. and Kaji,A. (2006) The ribosome-recycling step: consensus or controversy? *Trends Biochem. Sci.*, **31**, 143–149.
48. Brigotti,M., Petronini,P.G., Carnicelli,D., Alfieri,R.R., Bonelli,M.A., Borghetti,A.F. and Wheeler,K.P. (2003) Effects of osmolarity, ions and compatible osmolytes on cell-free protein synthesis. *Biochem. J.*, **369**, 369–374.
49. Uesono,Y. and Toh,E.A. (2002) Transient inhibition of translation initiation by osmotic stress. *J. Biol. Chem.*, **277**, 13848–13855.
50. Delot,E., King,L.M., Briggs,M.D., Wilcox,W.R. and Cohn,D.H. (1999) Trinucleotide expansion mutations in the cartilage oligomeric matrix protein (COMP) gene. *Hum. Mol. Genet.*, **8**, 123–128.
51. Russell,R.D. and Beckenbach,A.T. (2008) Recoding of translation in turtle mitochondrial genomes: programmed frameshift mutations and evidence of a modified genetic code. *J. Mol. Evol.*, **67**, 682–695.
52. Spanjaard,R.A. and van Duin,J. (1988) Translation of the sequence AGG-AGG yields 50% ribosomal frameshift. *Proc. Natl Acad. Sci. USA*, **85**, 7967–7971.